Feigenbaum cascade of discrete breathers in a model of DNA

P. Maniadis, B. S. Alexandrov, A. R. Bishop, and K. Ø. Rasmussen
Theoretical Division, Los Alamos National Laboratory, Los Alamos, New Mexico 87545, USA
(Received 24 August 2010; published 11 January 2011)

We demonstrate that period-doubled discrete breathers appear from the anticontinuum limit of the driven Peyrard-Bishop-Dauxois model of DNA. These novel breathers result from a stability overlap between subharmonic solutions of the driven Morse oscillator. Subharmonic breathers exist whenever a stability overlap is present within the Feigenbaum cascade to chaos and therefore an entire cascade of such breathers exists. This phenomenon is present in any driven lattice where the on-site potential admits subharmonic solutions. In DNA these breathers may have ramifications for cellular gene expression.

DOI: 10.1103/PhysRevE.83.011904 PACS number(s): 87.14.gk, 05.45.−a, 63.20.Pw

I. INTRODUCTION

Discrete breathers are spatially localized, temporally periodic excitations in nonlinear lattices [1]. While discrete breathers share many traits with solitons, they stand out because of their localization brought about by a delicate sensitivity to lattice discreteness. Discrete breathers have been ubiquitously studied in a wide variety of physical systems and have been the subject of intense theoretical and numerical scrutiny [1–5]. Although dissipation and driving are typically key experimental features, most of the theoretical and numerical studies have excluded such effects. Only quite recently have the effects of dissipation and driving been explicitly considered in numerical studies of discrete breathers [6].

Biomolecules represent a striking example of systems where the localization of discrete breathers has long been considered important, and where dissipation and driving cannot be ignored. DNA represents a specific biomolecular system where localization of energy in terms of strand-separation dynamics is emerging as a governing regulatory factor [7]. The Peyrard-Bishop-Dauxois (PBD) model of double-stranded DNA [8,9] is arguably the most successful model for describing this local pairing-unpairing (breathing) dynamics, since it reproduces a wide variety of experiments related to strand-separation dynamics [10]. Of particular importance is the role this model has played in demonstrating strong correlations between regulatory activity, such as protein binding and transcription, and the equilibrium propensity of double-stranded DNA for local strand separation [11–14]. Recently, this model was augmented to include a monochromatic drive in the THz frequency range, and was suggested to represent a simplified model for DNA dynamics in the presence of THz radiation [15]. In this recent work [15] the existence of discrete breathers oscillating at half the frequency of the drive was numerically observed, and it was argued that the existence and spontaneous generation of such breathing states may have significant ramifications for cellular gene expression. This argument has received some experimental support [16,17].

Here, we investigate these period-doubled breather excitations further, and show that they appear naturally from the anticontinuum limit [18] in systems of nonlinear oscillators where multistability occurs between various stages of the Feigenbaum period-doubling cascade. Although our study focuses on the PDB model, the observed phenomena are rather general and not limited to this specific system of nonlinear oscillators.

II. DNA MODEL

We consider the PBD model in the following form [15]:

$$m\ddot{y}_n = -U'(y_n) - W'(y_{n+1}, y_n) - W'(y_n, y_{n-1}) - m\gamma\dot{y}_n + F_0\cos\Omega t, \quad (1)$$

where the Morse potential

$$U(y_n) = D[\exp(-ay_n) - 1]^2$$

represents the hydrogen bonding of the complementary bases. Similarly,

$$W(y_n, y_{n-1}) = \frac{k}{2}(1 + \rho e^{-\beta(y_n + y_{n-1})})(y_n - y_{n-1})^2$$

represents the stacking energy between consecutive base pairs. The parameters D, a, and k in principle depend on the type of the base pair (A-T or G-C), but for simplicity we will consider homogeneous DNA in this study. The term $m\gamma\dot{y}_n$ is the drag caused by the solvent, while $F_0\cos\Omega t$ is the (THz) drive [19]. In this system, Eq. (1), the linear resonance frequency is given as $\Omega_0^2 = 2Da^2/m$.

In order to understand how period-doubled breathers oscillating at half the frequency, $\Omega/2$, of the drive can appear at the anticontinuum limit, we first study the nonlinear response of a single ($k = 0$) oscillator. For periodic driving the single oscillator supports periodic solutions with the period ($T = 2\pi/\Omega$) of the drive, and, due to the softness of the Morse potential, this oscillator also supports solutions with period nT, where n is any positive integer. These solutions are most simply studied at zero dissipation ($\gamma = 0$); we will then examine the modifications resulting when $\gamma \neq 0$. A Newton method [2] was used to track the solutions with periods T and $2T$. The Newton procedure was initiated for a very small driving amplitude ($F_0 \simeq 0$). The response of the system, namely the amplitude of the period T and $2T$ solutions, was followed as $|F_0|$ was increased.

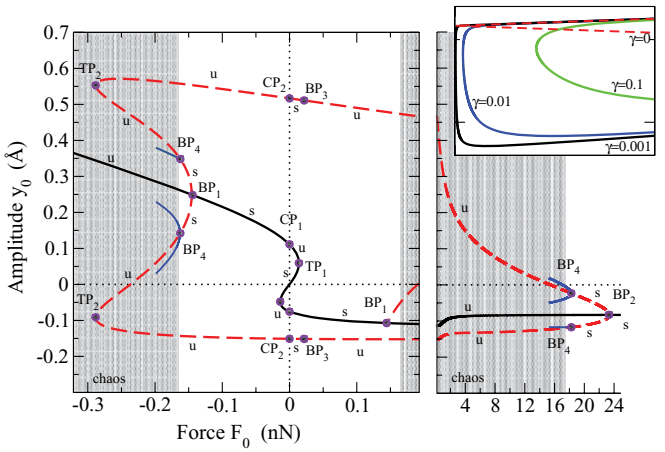

FIG. 1. (Color online) Nonlinear response manifold of a single oscillator driven at $\Omega = 7.0$ rad/ps ($<\Omega_0$). The NLRM for the period-T solutions (solid black line) and the period-doubled solutions (dashed red line) are shown together with parts of the NLRM for the period-$4T$ (solid blue line segments connected to BP_4) solutions. The stability of the various solutions is indicated by the letters placed in the vicinity of the lines ("s" for stable and "u" for unstable). Important turning points (TPs), bifurcation points (BPs), and crossing points (CPs) are shown by circles. Finally, the gray areas represent the chaotic regions that result from the Feigenbaum period-doubling cascades. The inset shows the behavior near CP_1 in the presence of dissipation. $\gamma = 0$ (dashed red line), $\gamma = 0.001$ ps^{-1}, $\gamma = 0.01$ ps^{-1}, and $\gamma = 0.1$ ps^{-1}.

A. Soft period-doubled breathers: $\Omega < \Omega_0$

In the above fashion we constructed the nonlinear response manifolds (NLRMs) [20] depicted for $\Omega = 7$ rad/ps in Fig. 1. The NLRM for the oscillations with period T is shown by the solid black line, while the dashed red line represents the NLRM for the period-doubled ($2T$) solutions. Finally, the blue line segments (connected to BP_4) represent parts of the NLRM for the period $4T$ solutions. The stability of the solutions can be obtained by Floquet stability analysis [2] and is indicated by the letters "s" (stable) and "u" (unstable) placed adjacent to the respective NLRMs. The stability of a given solution changes at the turning points (TPs), bifurcation points (BPs), or at the crossing points (CPs) of the NLRM. Since the Morse potential is asymmetric with respect to $y = 0$, the NLRMs lack symmetry with respect to a π-phase shift ($\pm F_0$) of the drive. However, an equivalence between the NLRM branches for F_0 and $-F_0$ remains, as is indicated by our labeling of the TPs, BPs, and CPs.

From Fig. 1 it can be noticed that, for a region of small positive force amplitudes F_0, the period-T solution is stable up to TP_1 ($F_0 \simeq \pm 14$ pN) and so is the period-doubled solution between CP_2 ($F_0 = 0$) and BP_3 ($F_0 \simeq 21.5$ pN). This means that in the region $0 < F_0 < 14$ pN both solutions are stable. A similar stability overlap can be observed for the regions $F_0 = 0$ to TP_1 (period T, $F_0 < 0$) and BP_4 to BP_1 (period doubled) when $\Omega < 5.5$ rad/ps (not shown in Fig. 1). The ramifications of these stability overlaps for the construction of discrete breathers is now clear. In the anticontinuum limit ($k = 0$) of N driven oscillators, we can construct solutions where $N - 1$ of the oscillators perform stable period-T oscillations, while

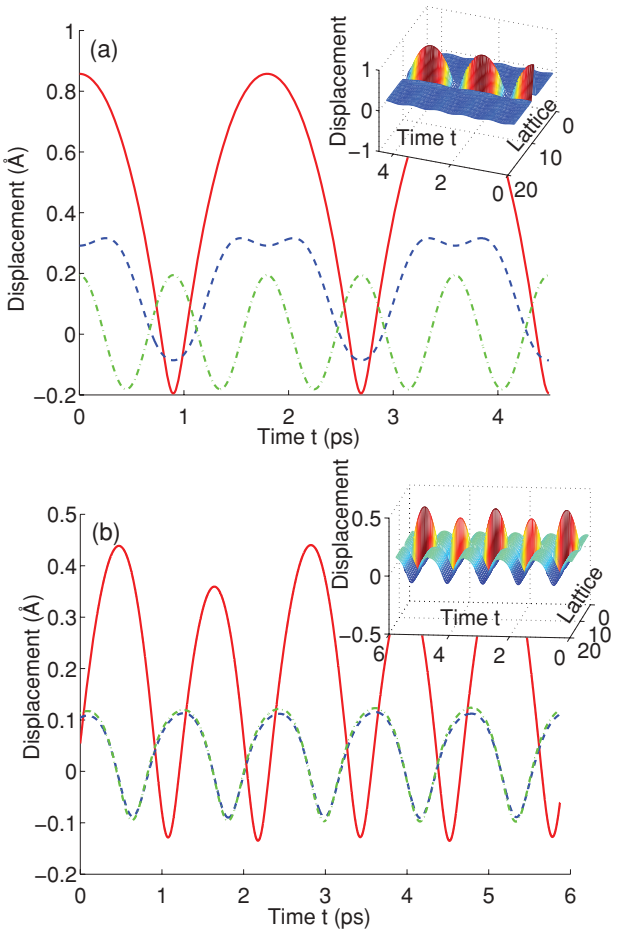

FIG. 2. (Color online) Illustration of period-doubled breathers. Shown are the central site y_0 of the breather (solid red lines) together with the closest neighbor sites y_1 (dashed blue lines) and y_2 (dashed-dotted green lines). For clarity, panel (a) shows $10y_1$ and $10y_2$, respectively. Panel (a) shows the period-doubled breather corresponding to the stability overlap shown in Fig. 1 ($\Omega = 7$ rad/ps and $\gamma = 0$) for $F_0 = 7.06$ pN and $k = 0.02$ eV Å^{-2}. Similarly, panel (b) shows a period-doubled breather for $\Omega = 5.35$ rad/ps, $\gamma = 1$ ps^{-1}, $F_0 = 115.6$ pN, and $k = 0.0065$ eV Å^{-2}. The insets shows the full spatiotemporal evolution of the period-doubled breathers.

the remaining oscillator resides stably in the period-doubled state. Performing standard numerical continuation [21] of this state to finite values of the coupling k will retain the stability of the solution and lead to a stable period-doubled discrete breather solution. Examples of such period-doubled breathers arising in each of the two described stability overlap regions are shown in Fig. 2. Figure 2(a) shows the period-doubled breather in the stability overlap region for $F_0 > 0$. It is clearly seen that the breather, which extends over five lattice sites, performs oscillations at exactly half the frequency of the background. The background is frequency locked to the drive at frequency Ω. Similarly, Fig. 2(b) shows the period-doubled breather that exists in the stability overlap region for $F_0 < 0$. The breather is more localized and its dynamical behavior is more complex. This breather roughly follows the background period-T oscillations and the period doubling occurs as a modulation of the breathing amplitude. For weak driving the

dynamics must be very similar to the undriven case, as is seen in Fig. 2(a). At stronger driving the dynamics is more dominated by the drive and becomes more intricate, as in the case of Fig. 2(b).

It should be noted that, in the absence of a stability overlap, unstable period-doubled breathers can of course still be constructed. An interesting example of this occurs for $F_0 <$ 23.3 nN, where Fig. 1 shows that the period-doubled solution is stable while the period-T solution is unstable. Close to BP_2 the period-T solution is very weakly unstable (the Floquet exponent is $\sim$1.04), so that a weakly unstable "dark" breather can be constructed in this region by positioning $N-1$ of the oscillators in the period-doubled states while the remaining oscillator is in the period-T state. We have found that numerical continuation of this state produces a weakly unstable "dark" breather that can be sustained for tens of periods.

The scenario described above generally holds also when dissipation is taken into account. The modifications to the NLRM caused by dissipation is thoroughly discussed for a different system of nonlinear equations in Ref. [6]. The main effect of dissipation occurs at the crossing points CP_1 and CP_2. For $\gamma = 0$ the period-T solutions are in phase with the drive when the response amplitude y_0 is below CP_1, but it is in antiphase (π-phase shifted) when y_0 is above CP_1. Similarly, the period-doubled solutions experience a π-phase shift at CP_2. The introduction of dissipation creates an additional phase shift between the drive and the response everywhere along the NLRM. This additional phase shift is largest close to the crossing points and causes the solution to disappear close to the crossing points (small $|F_0|$). This effect is illustrated in the inset of Fig. 1 for the CP_2 crossing point. It is clear that for weak dissipation the described stability scenario persists. However, as the dissipation increases, the stability overlap region is eventually lost and with it the stable period-doubled breathers.

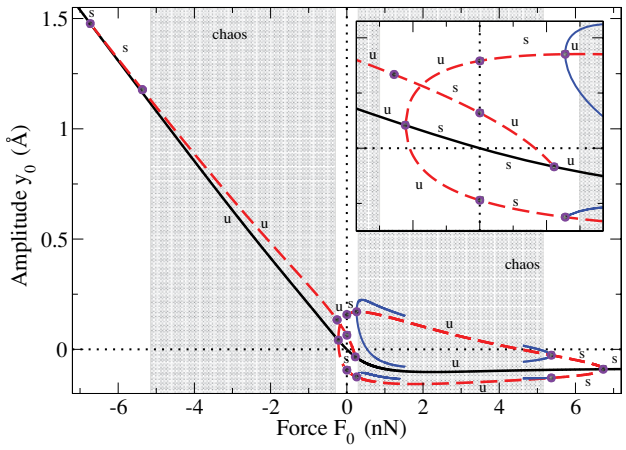

FIG. 3. (Color online) Nonlinear response manifold of a single oscillator driven at $\Omega = 13.194$ rad/ps ($>\Omega_0$). The NLRM for the period-T solution (solid black line) and the period-doubled solutions (dashed red line) are shown together with parts of the NLRM for the period-$4T$ (blue line segments) solutions. The stability of the solutions is indicated by the letters placed in the vicinity of the lines ("s" for stable and "u" for unstable). Important turning points, bifurcation points, and crossing points are shown by circles. Finally, the gray areas represent the chaotic regions that result from the Feigenbaum period-doubling cascades. A stability overlap can be observed in the vicinity of $F_0 = 0$. The inset shows a magnified version of the area between the chaotic regions.

B. Hard period-doubled breathers: $\Omega > \Omega_0$

Figure 3 shows the NLRM when the frequency of the drive ($\Omega = 13.194$ rad/ps) is larger than the linear resonance frequency of the on-site potential. In this case only a single, but larger, stability overlap between the period-T solution and the period-doubled solution exists in the vicinity of $F_0 = 0$. Again, the period-doubled breathers can be generated in this overlap region. It is noteworthy that for soft potentials, such as the Morse potential, ordinary period-T breathers cannot exist above the linear Ω_0 resonance frequency: This frequency region can only be accessed for hard potentials.

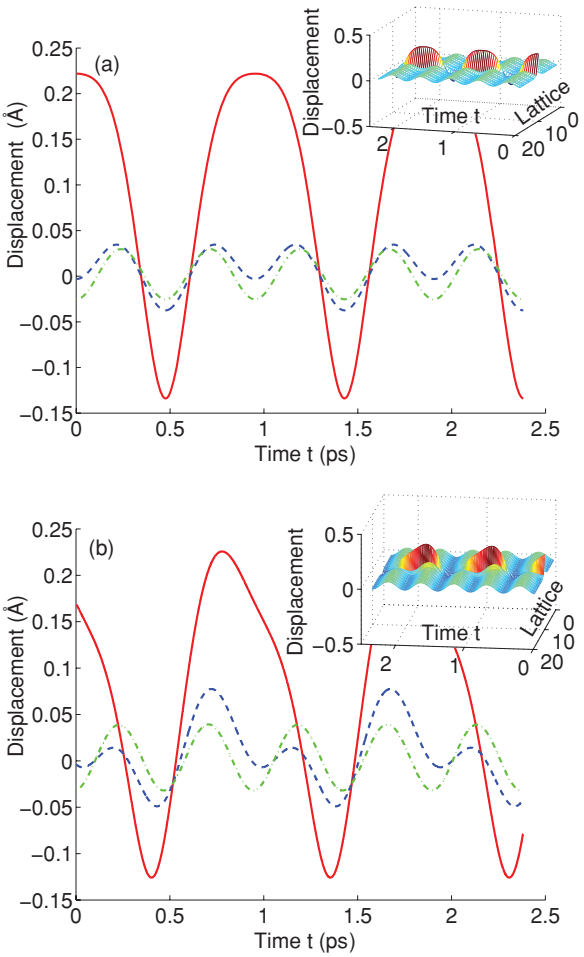

FIG. 4. (Color online) Illustration of period-doubled breathers. Shown are the central site y_0 of the breather (solid red lines) together with the closest neighbor sites y_1 (dashed blue lines), and y_2 (dashed-dotted green lines). Panel (a) shows the period-doubled breather corresponding to the stability overlap shown in Fig. 1 ($\Omega =$ 13.194 rad/ps and $\gamma = 0$) for $F_0 = 160$ pN and $k = 0.025$ eV Å^{-2}. Panel (b) demonstrates the effects of dissipation $\Omega = 13.194$ rad/ps, $\gamma = 1$ ps^{-1}, $F_0 = 209$ pN, and $k = 0.025$ eV Å^{-2}. The insets show the full spatiotemporal evolution of the period-doubled breathers.

Two examples of the period-doubled breathers for $\Omega = 13.194$ rad/ps are given in Fig. 4. Figure 4(a) shows a period-doubled breather in a dissipationless ($\gamma = 0$) system, and it is clear that the breather sites oscillate at half the frequency of the background, which is frequency locked to the drive. Similarly, Fig. 4(b) shows a period-doubled breather at strong dissipation $\gamma = 1$ ps^{-1}. The phase shift introduced by the dissipation is apparent.

III. DISCUSSION AND CONCLUSIONS

We have demonstrated the existence of a new kind of subharmonic discrete breather in driven lattices of coupled nonlinear oscillators. The phenomenon was illustrated within the driven PBD model, which consists of a lattice of coupled Morse oscillators. Specifically, we have shown that these breathers appear naturally from the anticontinuum limit in a fashion similar to familiar discrete breathers. We show that the subharmonic breathers arise from a stability overlap between subharmonic solutions of the single oscillator. This new kind of breather exists even when the frequency of the drive is above the linear resonance frequency of the soft on-site potential. Ordinary breather solutions do not exist in such cases for soft potentials.

Although we focused here on the stability overlap between the frequency locked solution and the period-doubled solution, it is clear that in the presence of a stability overlap the phenomena can occur between any of the subharmonic solutions in the Feigenbaum cascade. We have explicitly verified this by constructing stable periodic-nT ($n = 3,4,5$, and 6) breathers for small F_0 and k, in the case where $\Omega > \Omega_0$. In this fashion a cascade of subharmonic discrete breathers exists. The phenomenon is not specific to the system we have studied: It is present in any driven lattice of nonlinear oscillators where the on-site potential admits subharmonic solutions. The subharmonic breathers also exist in the presence of dissipation; it is, however, important to note that in this case the cascade is truncated.

The existence of the subharmonic breathers in DNA is potentially very important because this suggests that electromagnetic THz radiation can lead to the spontaneous generation of stable local strand separation in double-stranded DNA, and thereby could lead to modification in cellular gene expression by affecting transcription and other processes. Such effects have recently been experimentally observed [16,17]. Future extensions of our approach will include effects of gene sequence and other disorder, as well as temperature.

ACKNOWLEDGMENT

This research was carried out under the auspices of the National Nuclear Security Administration of the US Department of Energy at Los Alamos National Laboratory under Contract No. DE-AC52-06NA25396.

[1] S. Flach and A. V. Gorbach, Phys. Rep. **467**, 1 (2008).
[2] S. Aubry, Physica D **103**, 201 (1997).
[3] D. Chen, S. Aubry, and G. P. Tsironis, Phys. Rev. Lett. **77**, 4776 (1996).
[4] M. Johansson and S. Aubry, Nonlinearity **10**, 1151 (1997).
[5] M. Johansson and S. Aubry, Phys. Rev. E **61**, 5864 (2000).
[6] P. Maniadis and S. Flach, Europhys. Lett. **74**, 452 (2006).
[7] B. S. Alexandrov, V. Gelev, S. W. Yoo, L. B. Alexandrov, Y. Fukuyo, A. R. Bishop, K. Ø. Rasmussen, and A. Usheva, Nucleic Acids Res. **38**, 1790 (2010).
[8] M. Peyrard and A. R. Bishop, Phys. Rev. Lett. **62**, 2755 (1989).
[9] T. Dauxois, M. Peyrard, and A. R. Bishop, Phys. Rev. E **47**, R44 (1993).
[10] B. S. Alexandrov, N. K. Voulgarakis, K. Ø. Rasmussen, A. Usheva, and A. R. Bishop, J. Phys.: Condens. Matter **21**, 034107 (2009), and references therein.
[11] C. H. Choi, G. Kalosakas, K. O. Rasmussen, M. Hiromura, A. R. Bishop, and A. Usheva, Nucleic Acids Res. **32**, 1584 (2004).
[12] C. H. Chu, Z. Rapti, V. Gelev, B. S. Alexandrov, E. Park, J. Park, N. Horikoshi, A. Smerzi, K. O. Rasmussen, A. R. Bishop, and A. Usheva, Biophys. J. **95**, 597 (2008).
[13] B. S. Alexandrov, V. Gelev, Y. Monisova Y, L. B. Alexandrov, A. R. Bishop, K. Ø. Rasmussen, and A. Usheva, Nucleic Acids Res. **37**, 2405 (2009).
[14] B. S. Alexandrov, V. Gelev, S. W. Yoo, A. R. Bishop, K. Ø. Rasmussen, and A. Usheva, PLoS Comput. Biol. **5**, e1000313 (2009).
[15] B. S. Alexandrov, V. Gelev, A. R. Bishop, A. Usheva, and K. Ø. Rasmussen, Phys. Lett. A **374**, 1214 (2010).
[16] R. Shiurba *et al.*, Photoch. Photobio. Sci. **5**, 799 (2006).
[17] J. Bock, Y. Fukuyo, S. Kang, M. E. Phipps, L. B. Alexandrov, K. Ø. Rasmussen, A. R. Bishop, E. D. Rosen, J. S. Martinez, H.-T. Chen, G. Rodriguez, B. S. Alexandrov, and A. Usheva, PLoS ONE **5**, e15806 (2010).
[18] R. S. MacKay and S. Aubry, Nonlinearity **7**, 1623 (1994).
[19] In order to be consistent with prior work on DNA, we use the following parameters unless different values are explicitly given: $D = 0.05$ eV, $a = 4.2$ Å^{-1}, $k = 0.025$ eVÅ^{-2}, $\beta = 0.35$ Å^{-1}, $m = 300$ amu, and $\rho = 2$. With these parameters the linear resonance frequency is $\Omega_0 = \sqrt{2Da^2/m} = 7.54$ rad/ps, i.e., $\Omega_0/2\pi = 1.22$ THz.
[20] G. Kopidakis and S. Aubry, Phys. Rev. Lett. **84**, 3236 (2000).
[21] J. L. Marin and S. Aubry, Nonlinearity **9**, 1501 (1994).